

## **Natural aging of cool walls: impact on solar reflectance, sensitivity to thermal shocks and building energy needs**

Riccardo Paolini<sup>1,2\*</sup>, Andrea Zani<sup>1</sup>, Tiziana Poli<sup>1</sup>, Florian Antretter<sup>3</sup>, Michele Zinzi<sup>4</sup>

Accepted for publication in

**Energy and Buildings**

<https://doi.org/10.1016/j.enbuild.2017.08.017>

©2017. This manuscript version is made available under the CC-BY-NC-ND 4.0 license

<http://creativecommons.org/licenses/by-nc-nd/4.0/>

### **Disclaimer**

This document was prepared as an account of work sponsored by Politecnico di Milano & Agenzia delle Entrate (Italian Revenue Agency). While this document is believed to contain correct information, neither the Italian Government nor any agency thereof, nor the Research Institutions to which the authors are affiliated, nor any of their employees, makes any warranty, express or implied, or assumes any legal responsibility for the accuracy, completeness, or usefulness of any information, apparatus, product, or process disclosed, or represents that its use would not infringe privately owned rights. Reference herein to any specific commercial product process, or service by its trade name, trademark, manufacturer, or otherwise, does not necessarily constitute or imply its endorsement, recommendation, or favoring by the Italian Government or any agency thereof, or the Research Institutions to which the authors are affiliated. The views and opinions of authors expressed herein do not necessarily state or reflect those of the Italian Government or any agency thereof, or their Research Institutions.

---

<sup>1</sup> Politecnico di Milano, Department of Architecture, Built environment and Construction engineering

<sup>2</sup> The University of New South Wales, UNSW Built Environment

<sup>3</sup> Fraunhofer Institute for Building Physics, Department of Hygrothermics

<sup>4</sup> ENEA – UTEE-ERT Italian National Agency for New Technologies, Energy and Sustainable Economic Development

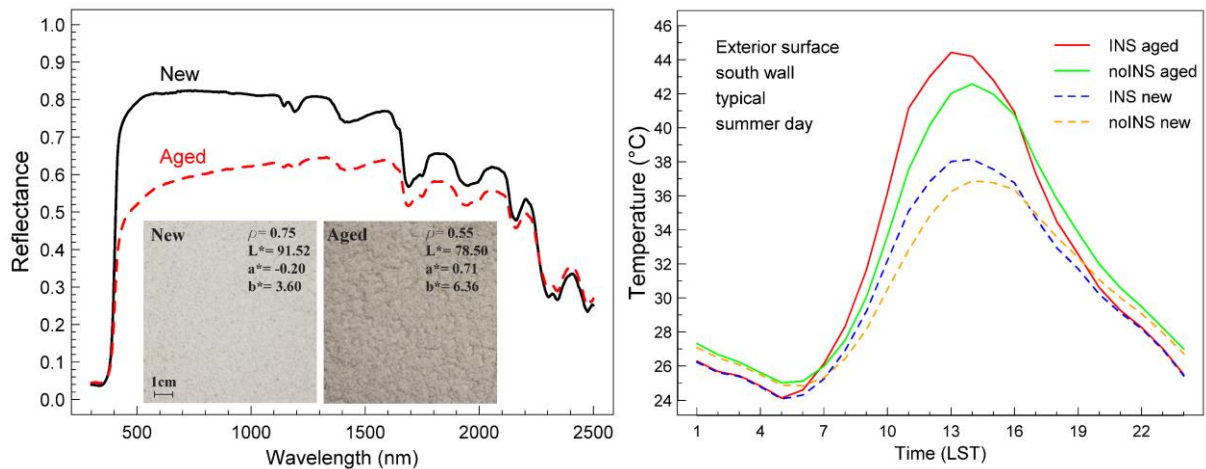
\* Corresponding author. Emails: [r.paolini@unsw.edu.au](mailto:r.paolini@unsw.edu.au), [RPaolini@LBL.gov](mailto:RPaolini@LBL.gov) – Current address: UNSW Built Environment, Red Centre West Wing, UNSW Sydney 2052, Sydney, Australia

## Abstract

Wall finishes with high solar reflectance and thermal emittance, commonly known as cool walls, can reduce the exterior surface temperatures of façades, and consequently the building cooling energy needs and power demand, and lower the sensitivity to degradation. Aging, though, may affect their performance. To investigate this risk, we exposed for four years in Milan, Italy, two series of façade finish coats, white and beige, facing north and south, in vertical and vertical-sheltered position, and we measured their solar spectral reflectance and thermal emittance before and after aging. The solar reflectance of the white finish coats drops from 0.75 to 0.55 in four years, and from 0.46 to 0.38 for the beige coats, while the thermal emittance is unchanged. Then, for a typical residential building with white walls, we computed that the cooling energy needs increase with walls aging by 5% and 11%, respectively, with or without exterior wall insulation. The exterior surface temperature is increased even by 6 °C, and the number of sudden surface temperature variations in one hour is boosted. Finally, the moisture content in the external layers is reduced, showing the impact on the heat and mass balance because of the uncertainty in solar absorption due to aging.

**Keywords:** solar reflectance; aging; soiling; cool walls; thermal shocks; building envelope; durability; cooling needs.

## Graphical Abstract



## Highlights

- We naturally aged for four years two types of façade finish coats in Milan, Italy.
- The solar reflectance of the white finish coats drops from 0.75 to 0.55.
- For a typical residential building, walls aging increases cooling needs by 5-11%.
- Aging increases the exterior surface temperature of insulated walls by up to 6 °C.
- Aging intensifies the sensitivity to thermal shocks of insulated white walls.

## 1. Introduction

Worldwide, the cooling energy consumption of buildings currently represents only 4.4% of the total consumption for heating and cooling. However, this figure is expected to increase to 35% by 2050, and up to 61% by 2100, because of the combination of global warming and

higher market penetration of air conditioning [1]. In some countries, such as India, the outlook is of a tenfold residential cooling energy consumption in 2050, with respect to current levels.

To reduce the cooling loads of buildings, several passive techniques have been pursued, including the exploitation of thermal storage, and night ventilation [2]. Moreover, it was soon understood that to tackle effectively the cooling loads it is necessary to act both on the building and the local urban climate scale. Therefore, during the last three decades, a wide range of building envelope technologies has been developed and tested with these objectives [3,4]. Among these technologies, highly reflective and emissive surfaces, widely known as cool surfaces, were proven to be an effective option, easy to be implemented [5–7]. Initially, the research on cool materials applications mostly concerned cool roofs [6,8], while more recent studies focused on applications for shading devices [9,10] and walls [11–14]. For instance, for a reference residential building in Mediterranean climate, an increase of the solar reflectance of the walls by 0.1 can provide cooling energy savings up to 2.9 kWh m<sup>-2</sup>, and reduce the indoor operative temperature by 1.1 °C of unconditioned buildings [12]. However, these documented benefits could be compromised by weathering and soiling [15–17], and biological growth [18,19]. There are some materials that exhibit self-cleaning features also over long periods, such as anatase added photoactive materials [20] or those that employ fluoropolymers [21,22]. In some cases, degradation causes the detachment of particles from the material surface, producing an apparent self-cleaning effect [23]. While there is information on the evolution over time of the optical-radiative response of roofing materials, it is not so for façade materials, for which the published data mostly concern their visual performance [24].

Here we show the results of a four-year natural exposure campaign of white and beige finish coats. We measured their solar reflectance ( $\rho_s$ ) and thermal emittance ( $\varepsilon$ ) before and after aging, and we computed the impact of aging of façades on (i) the heating and cooling loads of a typical residential building in Milan, Italy, (ii) the sensitivity to thermal shocks, and (iii) the moisture content within the wall layers.

## 2. Experiment

We selected from the market two standard finish coats (i.e., without self-cleaning features) that are commonly used for walls exterior insulation systems, one beige and another white, respectively with initial  $\rho_s$  equal to 0.46 and 0.75. The siloxane-based finish coat (with 0/1 mm sand) is 2 mm thick and it was applied onto a 4 mm thick base coat (i.e., cement mortar with 0/1 mm sand, with ~ 2% of acrylic resin as plasticizer). The two-coat system was laid on top of 10 cm × 10 cm fiber reinforced concrete slates used as a substrate (5 mm thick). From April 2012 to April 2016, we exposed in Milan, Italy (45° 28' 48" N; 9° 13' 46" E; 123 m above mean sea level), three replicates per product and per exposure condition, namely north and south, and vertical and vertical sheltered. The latter exposure condition refers to positioning the samples vertically underneath an overhang of 10 cm, which simulates a windowsill or roof gutter.

The exposure site is located on a rooftop, at 35 m above the street level and is equipped with a complete weather station [25]. During the aging campaign, the average

ambient temperature was of 15.39 °C (with 2<sup>nd</sup> and 98<sup>th</sup> percentiles equal to 1.6 °C and 31.2 °C, respectively), average wind speed of 1.6 m s<sup>-1</sup>, never exceeding 9 m s<sup>-1</sup>, and average yearly rainfall of 1176 mm. Milan's climate is cold during the winter and hot during summer, considerably drier than its surrounding non-urban adjacent areas [26].

The samples were retrieved, measured in the laboratory, and re-exposed on the metal racks at 3, 6, 12, 18, 24, 36, 42, and 48 months of natural aging. The spectral reflectance ( $\rho$ ) was measured with a PerkinElmer Lambda 950 spectrometer, equipped with a 150 mm integrating sphere, in the 300-2500 nm wavelength range, with a spectral resolution of 5 nm (with 25 samplings per wavelength). Each sample was measured in its center, characterizing an area of approximately 1 cm<sup>2</sup>. Then the average spectral curve was computed and broadband values were calculated starting from the spectral data, according to ISO 9050 [27]. The interlaboratory measurement uncertainty of this technique is equal or less than 0.020 [28,29]. The thermal emittance ( $\varepsilon$ ) was measured with the TIR 100-2 emissometer by Inglas, according to EN 15976 [30], performing five measurements per replicate. Thermal emittance measurements, considering all measurement methods, have an average uncertainty of  $\pm 0.02$  [29,31]. Given the thickness of the samples and their not perfectly smooth surface, the ASTM C 1371 method was not applicable neither in the original version nor in the 'slide method' variant [32,33]. We processed the average spectral curve, for each exposure condition, in the CIELab color space, composed by three color coordinates: L\*, lightness; a\*, hues from red to green; and b\*, hues from yellow to blue [34,35].

The capillary water absorption coefficient by partial immersion was measured on new and aged samples, after four years of exposure, according to ASTM C 1794 [36]. As the scope of this test is to observe changes with aging, to avoid known problems in repeatability and reproducibility [37,38], we performed the tests on all the samples in the same experimental session. In particular, for materials offering low water absorption, the deviation from interlaboratory median values may be even of 40 % [39], while within-laboratory deviations account for less than 10 % [37]. For the hygrothermal simulations, instead, we performed capillary water absorption tests of the same finish and base coat on a substrate of expanded polystyrene.

Finally, on a subset of three white coat replicates, exposed facing north, we performed two cleaning steps, similarly to the experiment by Levinson et al. on PVC roofing membranes [40]. We rinsed and brushed the samples, measured their  $\rho$ , and then brushed and washed them with a common soap based on sodium carbonate, measuring again  $\rho$  afterward.

### 3. Simulations

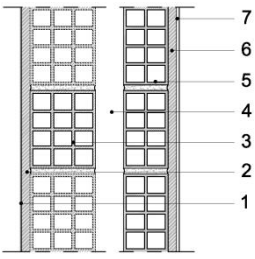
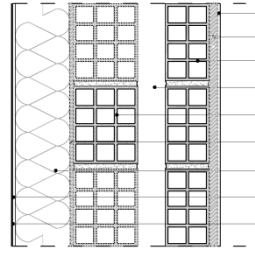
As a case study, we selected a residential isolated tower building (i.e., not surrounded by other buildings), that is representative of buildings with high solar access in Milan, Italy [41], namely those that could be mostly benefited by cool walls. Since the purpose of this study is to assess the impact of weathering and soiling of cool walls on the building hygrothermal and energy performance, we selected an isolated building, providing the upper bound of this variation. The ten-story building is 30 m high and 20.3 m  $\times$  20.3 m in plan, with a total net floor area of 3307 m<sup>2</sup>, façades perpendicular to the cardinal directions and four

windows per floor of 1.6 m × 1.7 m on each façade. We considered two case studies: non-retrofitted and retrofitted, the latter compliant with the current energy regulations in Italy [42] (Table 1). In both cases, we considered an aged roofing felt as a waterproofing layer on the flat roof (data from [16]). For the retrofitted case, we selected an External Thermal Insulation Composite System with rendering (ETICS), applied onto the existing wall substrate (Table 2).

Table 1. Building envelope features and surface area.

Building components	Orientation and area (m <sup>2</sup> )	Case 1: No insulation	Case 2: Insulated
Wall	Tot. 2014 N/E/S/W: 504	U = 0.49 W m <sup>-2</sup> K <sup>-1</sup> $\rho_{s,new}$ and $\rho_{s,aged}$ from experiment	U = 0.22 W m <sup>-2</sup> K <sup>-1</sup> $\rho_{s,new}$ and $\rho_{s,aged}$ from experiment
Roof	412	U = 0.56 W m <sup>-2</sup> K <sup>-1</sup> $\rho_s = 0.25$	U = 0.23 W m <sup>-2</sup> K <sup>-1</sup> $\rho_s = 0.25$
Floor	Tot. 3709 412	U = 0.51 W m <sup>-2</sup> K <sup>-1</sup>	U = 0.51 W m <sup>-2</sup> K <sup>-1</sup>
Floor over cellar	412	U = 0.52 W m <sup>-2</sup> K <sup>-1</sup>	U = 0.29 W m <sup>-2</sup> K <sup>-1</sup>
Window	Tot. 419 N: 109 E: 106 S: 98 E: 106	U = 2.9 W m <sup>-2</sup> K <sup>-1</sup> g-value = 0.75 + external shading system (roller shutter)	U = 1.4 W m <sup>-2</sup> K <sup>-1</sup> g-value = 0.57 + external shading system (roller shutter)

Table 2. External walls for the non-insulated and insulated case. The table reports thickness (t), bulk density ( $\gamma$ ), thermal conductivity in dry state at 10 °C ( $\lambda_{10^\circ\text{C,dry}}$ ), water capillary absorption coefficient ( $A_{w,24}$ ), and water vapor diffusion resistance factor ( $\mu$ ). In the ETICS, the base coat and the cement binder are the same (the base coat is reinforced with glass fiber mesh). Quantities and units are defined as in ISO 9346 [44].

	N°	Description	t (m)	$\gamma$ (kg m <sup>-3</sup> )	$\lambda_{10^\circ\text{C,dry}}$ (W m <sup>-1</sup> K <sup>-1</sup> )	$A_{w,24}$ (kg m <sup>-2</sup> s <sup>-0.5</sup> )	$\mu$ (d.u.)
	1	Finish coat	0.002	1600	1.28	0.0015	120
	2	Cement lime plaster	0.015	1900	0.8	0.017	19
	3	Aerated clay brick	0.12	600	0.12	0.095	16
	4	Air layer	0.05	1.3	0.28	-	1
	5	Aerated clay brick	0.08	600	0.12	0.095	16
	6	Cement lime plaster	0.015	1900	0.8	0.017	19
	7	Interior gypsum finish	0.005	850	0.2	0.287	8.3
	1	Finish coat	0.002	1600	1.28	0.0015	120
	2	Base coat	0.005	1900	0.8	0.0017	25
	3	Expanded polystyrene	0.1	30	0.04	-	50
	4	Cement-resin binder	0.005	1900	0.8	0.0017	25
	5	Aerated clay brick	0.12	600	0.12	0.095	16
	6	Air layer	0.05	1.3	0.28	-	1
	7	Aerated clay brick	0.08	600	0.12	0.095	16
	8	Cement lime plaster	0.015	1900	0.8	0.017	19
	9	Interior gypsum finish	0.005	850	0.2	0.287	8.3

The capillary water absorption coefficient of the walls finish coat and the solar reflectance and thermal emittance are the values achieved with the experimental activity of this study. The other material properties are from the WUFI database, derived from measurements of samples representative of typical building materials carried out at certified laboratories and consistent with the data from the MASEA database [43].

The set point for heating is of 20 °C from 8 am to 10 pm and of 17 °C during the night hours, during the heating season, while the set point for cooling is of 26 °C without schedule, as defined by the Italian technical regulation [45]. We set the air changes per hour (ACH) equal to 2 during night hours in the cooling season and equal to 0.5 for the rest of the time. These values include natural ventilation and infiltrations/exfiltrations and are in line with data from a survey in residential buildings in Europe [46]. The loads are defined in Table 3. We simulated both cases with the white finish coat as new and as aged, namely with  $\rho_s$  before and after four years of natural exposure.

Table. 3. Occupancy and internal heat and moisture gains, for a total net floor area of 3307 m<sup>2</sup>.

	<b>N° of people during day</b>	<b>Heat (W)</b>	<b>Moisture (g h<sup>-1</sup>)</b>	<b>CO<sub>2</sub> (g h<sup>-1</sup>)</b>	<b>Human activity (Met)</b>
Total internal loads	130 (Max) 95 (Medium)	22715	14787	3600	0.97

We performed the building hygrothermal simulations (3-D) with the software model WUFI Plus 3.0.3 [47–49], that computes dynamic heat and moisture balance, with the finite control volumes method, coupling heat transfer with liquid and vapor moisture transport in porous media. WUFI Plus was validated within the context of IEA Annex 41 [48] and tested with measurements in the laboratory and experimental buildings [49–51]. To compute the heat and moisture transport through the walls, we used the 1-D model interface WUFI 5.3, with a mesh of 500 finite control volumes, and the indoor conditions provided by the building model. We initialized the simulation with a temperature of 15 °C and relative humidity of 80% across the building component (for both building and 1-D simulations). In this case, our purpose is to consider the building and component performance in regime conditions, elapsed the initial high moisture content due to the construction phase. We used the weather data collected by a station at exposure site [25], from 2011 to 2016, considering the results for only the last five years, and using the first year as initialization. We assessed also the sensitivity to thermal shocks, that, together with cyclic temperature variations, are a relevant degradation mode for ETICS [52,53]. We computed the number of times when the surface temperature of walls with exterior insulation is equal to or greater than 10 °C, 15 °C, or 20 °C, similarly to Daniotti et al. [54]. We did not consider a single threshold, as there is no consensus on the value beyond which fatigue occurs. We simulated also a wall with  $\rho_s$  of 0.30, as a reference, because it is the lowest accepted value in warm climates to prevent early failures [55].

## 4. Results and discussion

### 4.1 Experimental results

During the first three months of natural exposure, both white and beige finish coats lost in average 0.02-0.03 in  $\rho_s$ , with small differences between north and south (Figure 1a).

Then, every six months,  $\rho_s$  of the white finish coat dropped by approximately 0.03, with the most substantial decreases occurring during the heating season, while stability was reached during the last year. After 48 months, losses in  $\rho_s$  for the beige and the white finish coats account, respectively, to 0.08 and 0.20.  $\varepsilon$ , instead, is unaffected by aging and equal to 0.94 (with a standard deviation of 0.005) for both beige and white finish coats. Aging strongly affects the lightness, with a smaller impact on the red/green and yellow/blue coordinates (Figure 1b, c, d), while the intensity of the effects does not seem to be highly influenced by orientation and positioning. Lightness steadily decreased during the first three years and it became almost stable in the last year, with the maximum loss equal to 16 for the white sheltered south facing samples, while the beige samples had a maximum loss not exceeding 5, with  $\Delta L^*$  fluctuating between -3.5 and -4.5.

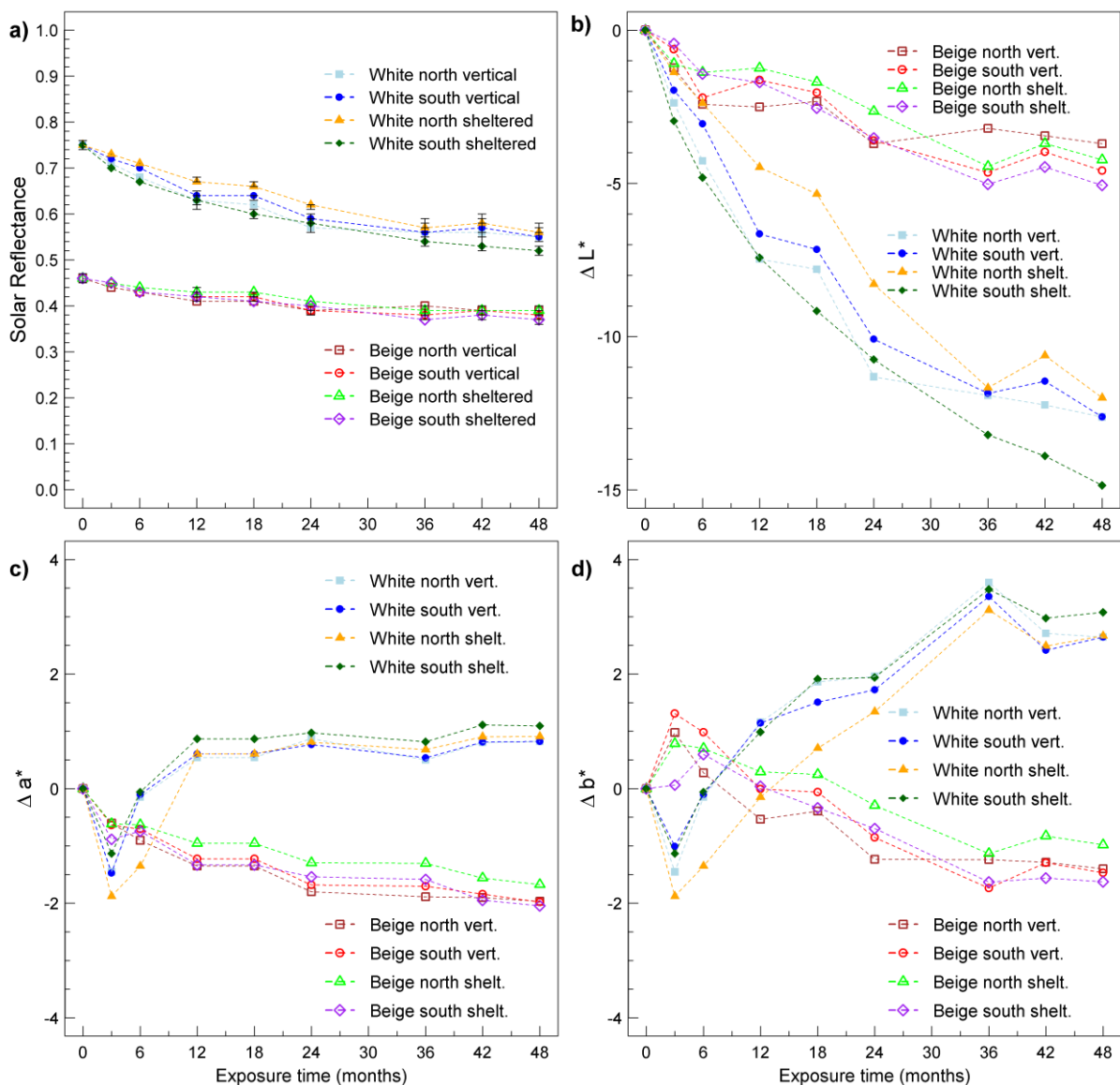


Figure 1. (a) Solar reflectance and variation in (b) lightness ( $\Delta L^*$ ), (c) red/green coordinate ( $\Delta a^*$ ) and (d) yellow/blue coordinate ( $\Delta b^*$ ) for the white and beige finish coat samples.

After the first 3 months, the sign of  $\Delta a^*$  and  $\Delta b^*$  of the white samples changed, and with their surface becoming redder and yellower after the first year. Red/green coordinates



variation ( $\Delta a^*$ ) both increased by approximately +1, while the increment in yellow/blue coordinates was of +3. The  $\Delta a^*$  and  $\Delta b^*$  at six months of exposure for the beige finish coats were within  $\pm 2$ , similarly to what observed by Diamanti et al. on colored mortars containing  $\text{TiO}_2$  with red and brown pigments [24]. Then, they reached a stable value of approximately -2 after four years. Trials determined that  $\Delta = 1$  is the minimum threshold for 50 % color match acceptability [56] and  $\Delta = 2$  for 100 % detection of color mismatch in vitro [57], while differences of approximately 3 units are perceived in vivo [58]. Therefore, both variations for color coordinates in our experiment can be regarded as unperceivable or barely perceivable, but of limited importance, while  $\Delta L^*$  greatly impacts the aesthetic performance (Figure 2).

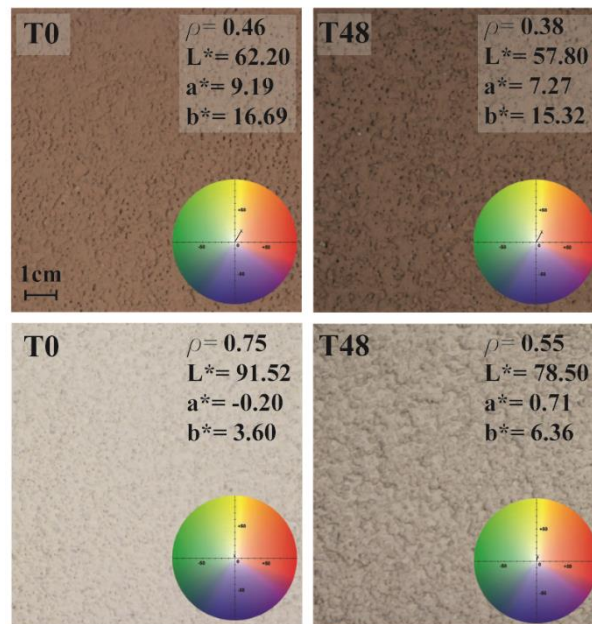


Figure 2. Aspect of the new and aged samples (after 48 months of exposure), and synthetic parameters.

The inflection points in the aged spectra at approximately 420 nm and 600 nm is compatible with the degradation of the binder of the finish coat (Figure 3b), because of UV-Vis aging (blue wavelengths are also reported to cause aging in addition to UV [21]). The same is suggested by the slight yellowing, too (Figure 1b and 2). The alteration in the Vis and the first portion of the NIR is also compatible with the impact of humic acid [15]. There is no visual evidence of significant physical disintegration (Figure 2), which could have produced a recovery in  $\rho$  [23], and the trend of  $\rho_s$  is, in fact, monotonic, excluded some small fluctuations (Figure 1). By image magnification, we observed no sign of biological growth and we do not recognize the spectral features in the Vis region typical of fungi/algae [40].

The capillary water absorption tests did not show any relevant variation in the water absorption coefficient upon four years of natural aging (of less than  $0.0005 \text{ kg m}^{-2} \text{ s}^{-0.5}$ , that is within the experimental error). However, this is not indicative of the absence of changes, as clogging by salts or dust is known to alter the moisture transport properties [59], as well as carbonation in cement-based materials, that may reduce the water absorption [60]. These phenomena may compensate or even exceed the possible increase in capillarity due to



physical aging. Therefore, we cannot draw any conclusion on the causes of the absence of relevant changes in water absorption.

One of the most frequent alterations in the optical response of cement-based materials is due to carbonation and efflorescence, but it is a transient effect as calcium carbonate and salts are highly soluble and tend to be rain washed [61]. Pure calcite is highly reflective at all wavelengths between 800 nm and 2500 nm [62], and its purity and particle size highly influence its reflectivity [63,64]. Therefore, carbonation typically yields to an increase in  $\rho$ , that we do not observe in this case, although a slight increase between 2300 nm and 2500 nm upon aging is actually compatible with a residual of calcium carbonate (Figure 3). Thus, we argue that if carbonation and salt transport occur, their impact is not prevalent and it has no relevant impact on solar reflectance in this case.

The fact that the samples just appear darker, while their color is almost unchanged (Figures 1 and 2), suggests that the most relevant contribution to the performance loss might be attributed to black carbon, which is known to decrease almost unselectively the reflectance of exposed surfaces [15]. The impact of black carbon can be recognized more clearly in the aged spectra (Figure 3). The broadband reduction in reflectance is compatible with the optical absorption of soot [65]. In fact, weathering and soiling affect  $\rho$  between 300 nm and 1500 nm in the Vis and the first part of NIR band, while in the UV and after 1500 nm  $\rho$  is subject to less relevant losses [16].

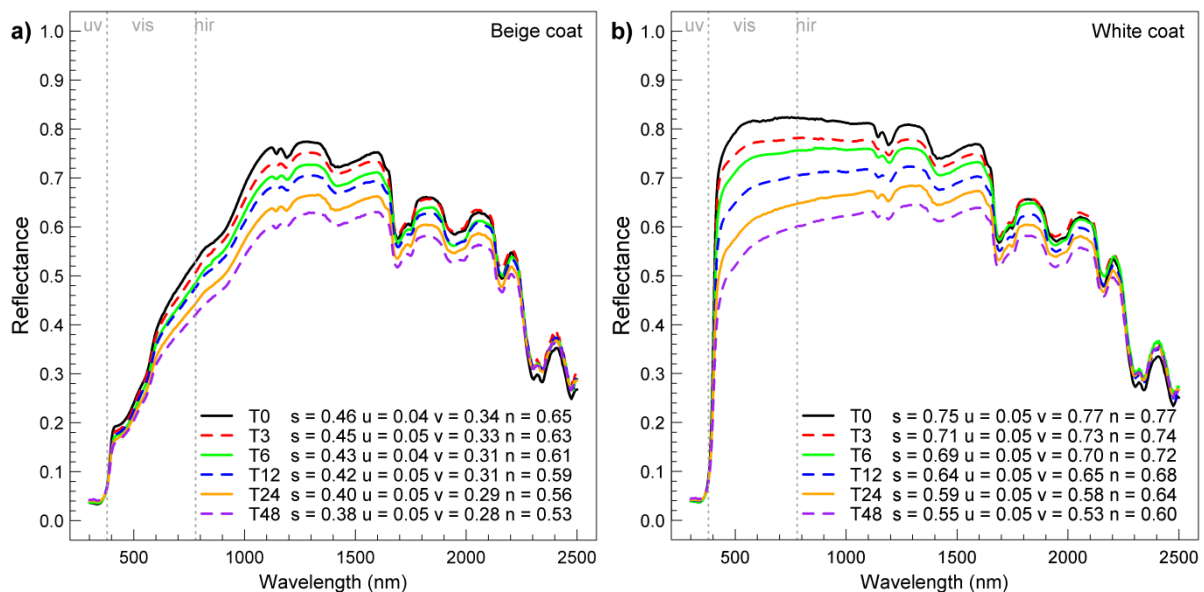


Figure 3. Average spectral reflectance for all orientations and exposure conditions of a) beige and b) white finish coat (the measurements at 18, 36, and 42 months are not displayed).

The prevalence of the contribution of soot to the broadband performance loss and its spectral features is confirmed by the cleaning test on the north exposed white samples (Figure 4). In Milan, black carbon mostly originates from diesel exhausts from vehicular traffic [66], as domestic heating is provided almost only with natural gas, that produces  $\text{NO}_x$  [67]. The average concentrations, among the highest in Europe [68], during winter, exceed  $10 \mu\text{g m}^{-3}$  at street level [69,70], while in summer they are lower than  $3 \mu\text{g m}^{-3}$ . However, the

concentrations of carbon monoxide (CO) and fine particulate matter such as PM<sub>2.5</sub> at our exposure site are likely to be very different from those at street level, or in general in the plurality of urban microenvironments [71].

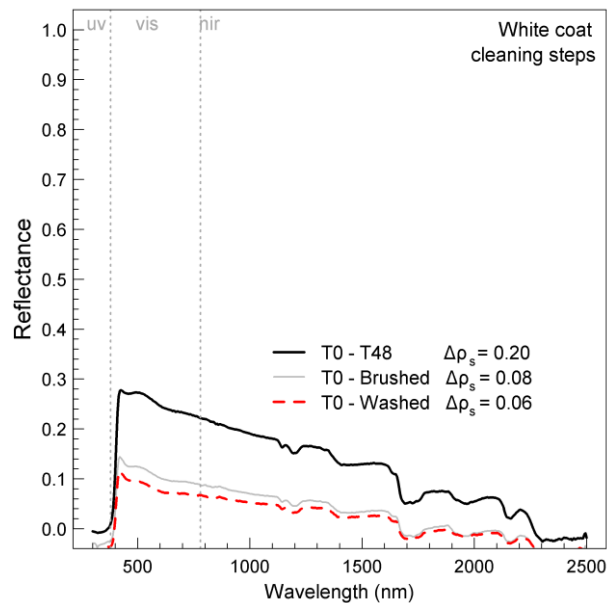


Figure 4. Solar spectral reflectance loss, with respect to the initial condition of the north facing white coat samples after four years of natural aging (T0 - T48), then after rinsing and brushing (T0 - Brushed), and after an additional cycle of brushing and washing with sodium carbonate soap (T0 - Washed).

In fact, the concentration of pollutants decreases with height, because of the location of the main sources and of the reduced removal by the wind, which is itself reduced within the urban canopy layer to even one-fifth the values over the canopy [72]. For instance, Di Sabatino et al. computed CO concentrations at street level that are ten times those over the canopy [72], in addition to spatial variations in the horizontal plane depending on the distance from the source. Given that the samples were exposed on a rooftop, the reflectance losses that we found can be regarded as representative of the average situation. A stronger impact of soiling on the reflectance of cool walls is expected for lower floors at the most polluted locations within the urban area, such as crossroads with traffic lights. Moreover, the morphology of the building façade (due to balconies, overhangs or other 3-D features) can deeply impact the soiling patterns, and the rain-wash (e.g., Figure 5).



Figure 5. The façade of a building in Milan, showing the impact of morphology on soiling (please note that this façade is not covered with the materials investigated in this study. It is shown with the only purpose of demonstrating soiling patterns on complex façades).

#### 4.2 Simulations results

For the considered non-retrofitted reference building, a loss of 0.20 in  $\rho_s$  increases the specific cooling needs (referred to the net floor area) by  $2 \text{ kWh m}^{-2} \text{ y}^{-1}$ , and by  $0.8 \text{ kWh m}^{-2} \text{ y}^{-1}$  for the retrofitted case, namely, respectively, the 11% and 5% of the initial energy needs.

Since the relationship between solar reflectance of the building envelope and cooling energy needs is linear [6], the measurement uncertainty of 0.02 [28,29], which in our case is one tenth of the observed reflectance loss, would yield to a difference in cooling load of  $0.16 \text{ kWh m}^{-2} \text{ y}^{-1}$  for the insulated case and  $0.08 \text{ kWh m}^{-2} \text{ y}^{-1}$  for the uninsulated case. However, these are acceptable values that account for a small fraction of the overall uncertainty of building energy performance, typically of greater magnitude [73,74].

We compute, instead, a small reduction of the initial heating need, of 4% and 2% for the non-retrofitted and retrofitted buildings (Figure 6a). Aging of the walls finishing also increases the power demand, especially in the intermediate power demand range, when the number of hours when there is cooling demand is increased (Figure 6b). The cooling savings reductions due to aging are in line with what Zinzi computed for a residential building in Marseille [12] (i.e., specific cooling savings of  $0.2\text{-}0.4 \text{ kWh m}^{-2} \text{ y}^{-1}$  for an insulated building, and of 0.6 for a non-insulated building per 0.1  $\rho_s$  increase). The variations we computed are relatively small, but they contribute to increasing the uncertainty in building energy simulation. Thus, aged values for the solar reflectance of walls shall be considered.

However, the most relevant aspect is probably the increase in exterior surface temperatures. In fact, a white aged ETICS can be  $6 \text{ }^\circ\text{C}$  hotter than when new, considering a typical hot summer day (Figure 7a). Moreover, the cumulative distribution is greatly impacted (Figure 7b).

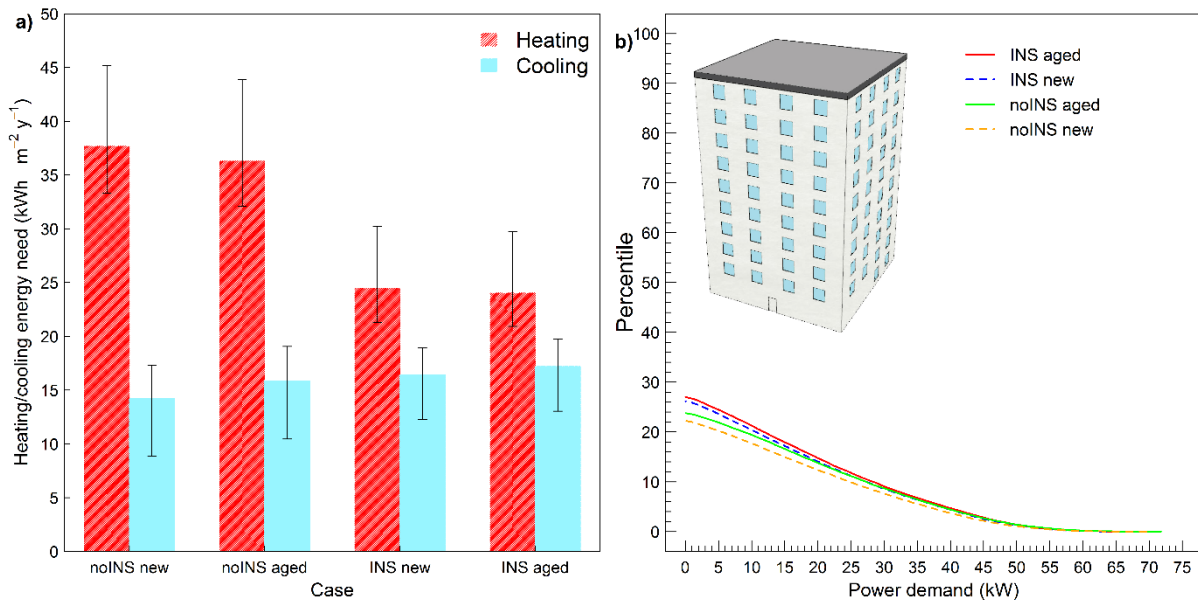


Figure 6. a) Five year averaged specific heating and cooling needs with or without insulation, with the white finish coat as new or aged. The whiskers identify the maximum and minimum yearly values. b) Percentiles distribution of the cooling power demand during five years. A sketch of the modeled building is embedded in figure b).

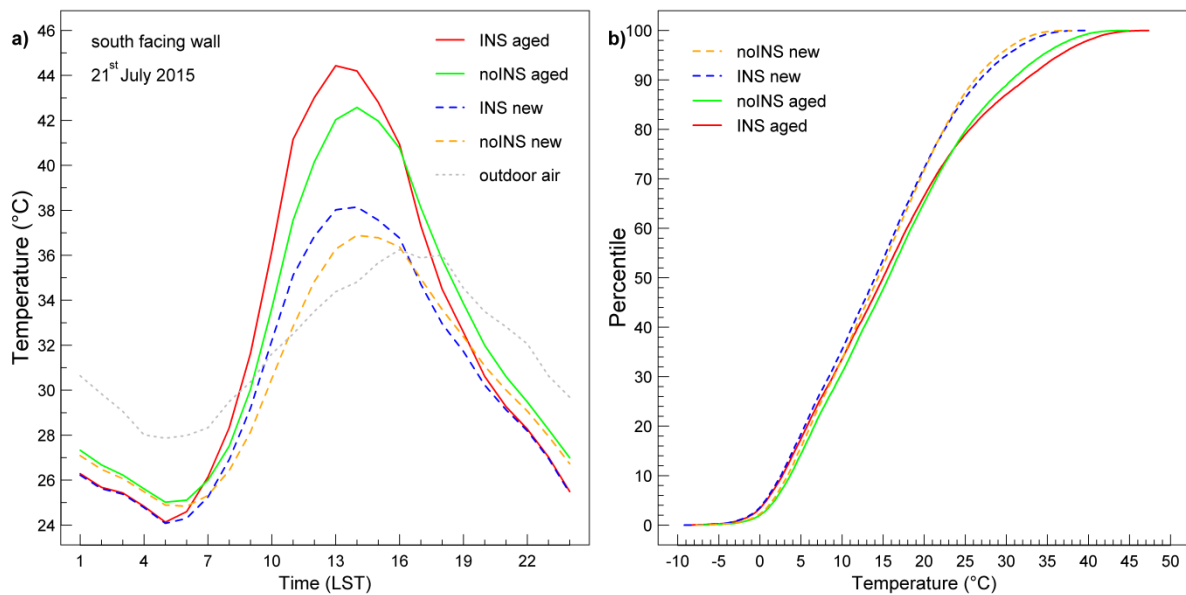


Figure 7. Exterior surface temperature for a south facing wall when insulated or non-insulated, with a new or aged white finish coat: (a) daily course during a typical hot summer day; (b) percentiles distribution during five years.

With aging, for the non-insulated wall, the 98<sup>th</sup> percentile gets from 32 °C to 38 °C, while for the wall with ETICS the variation is from 33 °C to 40 °C, implying an increase in the magnitude of thermal stress-strain cycles.

The increase in solar absorption produced by aging also causes an increase in the number of sudden temperature variations in one hour (Figure 8), which is a proxy of the sensitivity to thermal shocks. A new white ETICS, facing south, is almost unaffected by sudden variations in the boundary conditions, with only 19 times/year with a surface

temperature variation exceeding 10 °C, and no severe events. When aged, instead, the white ETICS starts to show some intense sudden surface temperature variations. However, the most intense events ( $\Delta T \geq 20$  °C in 1 h) are more frequent for east facing walls.

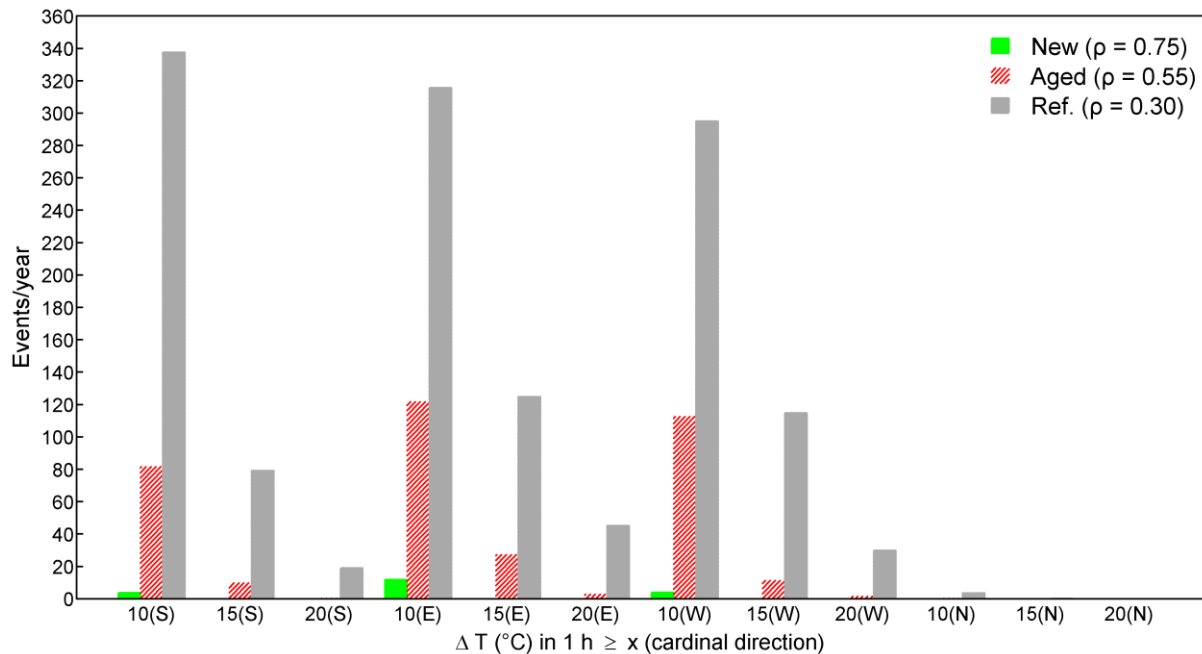


Figure 8. Sensitivity to hygrothermal shocks: number of events per year when the surface temperature varies in one hour by a value equal to or greater than 10 °C, 15 °C, or 20 °C, per cardinal direction (S, E, W, N).  $\rho_s$  is given for an ETICS with white new and aged finish coat, and a dark finish coat.

Although these are a minimal fraction ( $\sim 6\%$ ) of the events computed for the ETICS with low  $\rho_s$  (reported to be subject to early failures), this might reduce the service life of the system. The fact that the most affected orientation is east – and not south – can be explained by considering that during the night condensation occurs on highly insulated walls, and the condensed and adsorbed water quickly evaporates at sunrise. Inversely, this occurs at sunset for west facing walls. This and the influence of wind also explain the different ratios between the number of events for coatings with different  $\rho_s$ . Differences in the frequency of thermal shocks depending on wall orientation are also connected to the wind-driven rain load:  $\sim 100$  m  $y^{-1}$  on walls facing south, 80 mm  $y^{-1}$  west, and 190 mm  $y^{-1}$  east. Not surprisingly, north facing walls are unaffected by thermal shocks. Finally, considering the initial  $\rho_s$  in simulations would yield to a peak overestimation in the moisture content in the base coat of the ETICS of 20 kg  $m^{-3}$ , and a median overestimation of 5 kg  $m^{-3}$  (Figure 9). The overestimation in the most external 1 cm of the thermal insulation, instead, is always lower than 2 kg  $m^{-3}$ . Similar figures are computed for east and west facing walls, while for north facing walls the differences are about 60% of those computed for south walls. These small variations already yield to a different surface latent heat balance, and therefore to different heat losses. A robust estimation of the moisture contents within the layers that are mostly affected by degradation processes is needed to assess the sensitivity of building envelope components to critical events such as freeze-thaw cycles, and estimate their service life.

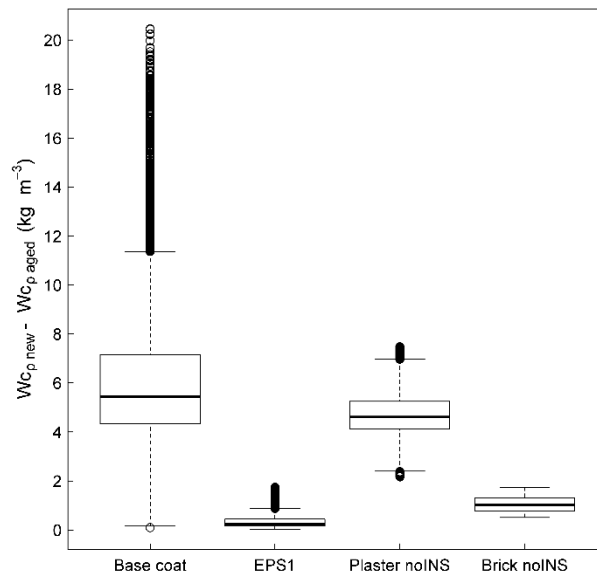


Figure 9. Difference between the moisture content computed with a new or aged finish coat, for the base coat of the ETICS, the first 1 cm from the exterior of the insulation, and the exterior plaster and exterior brick layer of a non-insulated wall.

## 7. Conclusions

Cool walls can reduce the exterior surface temperatures of façades and thus the cooling needs, and the sensitivity to degradation mechanisms, but aging may compromise their performance. To study this problem, we exposed for four years in Milan, Italy, white and beige finish coats, of the type that is commonly used for exterior insulation systems (ETICS).

The lightness of the white finish coats is greatly impacted by soiling, with losses up to 16, while the maximum  $\Delta L^*$  for beige finish coats is of 5, with small changes in color coordinates. The white finish coats lose 0.20 in  $\rho_s$  in four years, while the beige coats lose 0.08, without variations in  $\varepsilon$ . The four exposure conditions (i.e., north/south and vertical/vertical-sheltered) yielded to differences in  $\rho_s$  loss not exceeding 0.03.

For a typical residential building in Milan, whose façades are finished with the white coat, we computed that these reflectance losses may cause an increase of the specific cooling needs by 1.6 kWh m<sup>-2</sup> for the non-retrofitted building, and 0.8 kWh m<sup>-2</sup> for the retrofitted one. With aging, the peak exterior surface temperature is increased even by 6 °C for the aged ETICS, and the 98<sup>th</sup> percentile of the surface temperature gets from 33 °C to 40 °C, that may boost the magnitude of thermal stress-strain cycles. Moreover, a new white ETICS, facing south, is almost unaffected by sudden variations in the boundary conditions. When aged, instead, the white ETICS starts to show some intense sudden surface temperature variations, which may affect its service life. Finally, we have shown that considering the initial  $\rho_s$  yields to an overestimation in the moisture content of the exterior layers of a wall.

In this study, we have shown that while the impact of weathering and soiling of cool walls on the building energy needs might be modest, aged values should be anyway used in simulations. Moreover, the loss in solar reflectance of cool walls, caused by aging, may reduce their service life. Developing materials with effective self-cleaning features over the

long-term is important to improve the durability of built assets and reduce their life cycle environmental impact. Reducing the uncertainty in the estimation of the heat and moisture fluxes is relevant, for instance, to approach a multi-physics assessment of the performance over time of building envelopes and to design durable buildings.

## Acknowledgments

This work was supported by Politecnico di Milano & Agenzia delle Entrate (Italian Revenue Agency) with the project “Cinque per mille junior - Rivestimenti fluorurati avanzati per superfici edilizie ad alte prestazioni”. We thank the staff of Osservatorio Meteo Milano Duomo for the validation of weather data used for the numerical simulations. We thankfully acknowledge Chiara Ferrari and Alberto Muscio (of the University of Modena and Reggio Emilia) for the measurements of thermal emittance. We thank Prof. Hashem Akbari (of Concordia University) for valuable suggestions.

## References

- [1] M. Santamouris, Cooling the buildings – past, present and future, *Energy Build.* 128 (2016) 617–638. doi:10.1016/j.enbuild.2016.07.034.
- [2] M. Santamouris, D. Asimakopoulos, eds., *Passive cooling of buildings*, James & James (Science Publisher) Ltd., London, UK, 1996.
- [3] H. Akbari, D. Kolokotsa, Three decades of urban heat islands and mitigation technologies research, *Energy Build.* 133 (2016) 834–842. doi:10.1016/j.enbuild.2016.09.067.
- [4] H. Akbari, C. Cartalis, D. Kolokotsa, A. Muscio, A.L. Pisello, F. Rossi, M. Santamouris, A. Synnefa, N.H. Wong, M. Zinzi, Local climate change and urban heat island mitigation techniques – the state of the art, *J. Civ. Eng. Manag.* 22 (2015) 1–16. doi:10.3846/13923730.2015.1111934.
- [5] A.H. Rosenfeld, H. Akbari, J.J. Romm, M. Pomerantz, Cool communities: strategies for heat island mitigation and smog reduction, 1998. doi:10.1016/S0378-7788(97)00063-7.
- [6] A. Synnefa, M. Santamouris, H. Akbari, Estimating the effect of using cool coatings on energy loads and thermal comfort in residential buildings in various climatic conditions, *Energy Build.* 39 (2007) 1167–1174. doi:10.1016/j.enbuild.2007.01.004.
- [7] M. Santamouris, L. Ding, F. Fiorito, P. Oldfield, P. Osmond, R. Paolini, D. Prasad, A. Synnefa, Passive and Active Cooling for the Outdoor Built Environment – Analysis and Assessment of the Cooling Potential of Mitigation Technologies Using Performance Data from 220 Large Scale Projects, *Sol. Energy*. In press (2016). doi:10.1016/j.solener.2016.12.006.
- [8] H. Akbari, R. Levinson, L. Rainer, Monitoring the energy-use effects of cool roofs on California commercial buildings, *Energy Build.* 37 (2005) 1007–1016. doi:10.1016/j.enbuild.2004.11.013.
- [9] M. Zinzi, E. Carnielo, S. Agnoli, Characterization and assessment of cool coloured solar protection devices for Mediterranean residential buildings application, *Energy Build.* 50 (2012) 111–119. doi:10.1016/j.enbuild.2012.03.031.
- [10] A. Pisello, A. Laura, Experimental Analysis of Cool Traditional Solar Shading Systems for Residential Buildings, *Energies*. 8 (2015) 2197–2210. doi:10.3390/en8032197.
- [11] M. Zinzi, Characterisation and assessment of near infrared reflective paintings for building facade applications, *Energy Build.* 114 (2015) 206–213. doi:10.1016/j.enbuild.2015.05.048.
- [12] M. Zinzi, Exploring the potentialities of cool facades to improve the thermal response of Mediterranean residential buildings, *Sol. Energy*. 135 (2016) 386–397. doi:10.1016/j.solener.2016.06.021.
- [13] M. Doya, E. Bozonnet, F. Allard, Experimental measurement of cool facades’ performance in a dense urban environment, in: *Energy Build.*, 2012: pp. 42–50. doi:10.1016/j.enbuild.2011.11.001.
- [14] G.M. Revel, M. Martarelli, M. Emiliani, L. Celotti, R. Nadalini, A. De Ferrari, S. Hermanns, E. Beckers, Cool products for building envelope – Part II: Experimental and numerical evaluation of thermal performances, *Sol. Energy*. 105 (2014) 780–791. doi:10.1016/j.solener.2014.02.035.
- [15] M. Sleiman, T.W. Kirchstetter, P. Berdahl, H.E. Gilbert, S. Quelen, L. Marlot, C. V. Preble, S. Chen, A. Montalbano, O. Rosseler, H. Akbari, R. Levinson, H. Destailats, Soiling of building envelope surfaces and its effect on solar reflectance – Part II: Development of an accelerated aging method for roofing materials, *Sol. Energy Mater. Sol. Cells*. 122 (2014) 271–281. doi:10.1016/j.solmat.2013.11.028.



- [16] R. Paolini, M. Zinzi, T. Poli, E. Carnielo, A.G. Mainini, Effect of ageing on solar spectral reflectance of roofing membranes: natural exposure in Roma and Milano and the impact on the energy needs of commercial buildings, *Energy Build.* 84 (2014) 333–343. doi:10.1016/j.enbuild.2014.08.008.
- [17] G.M. Revel, M. Martarelli, M.Á. Bengochea, A. Gozalbo, M.J. Orts, A. Gaki, M. Gregou, M. Taxiarchou, A. Bianchin, M. Emiliani, Nanobased coatings with improved NIR reflecting properties for building envelope materials: Development and natural aging effect measurement, *Cem. Concr. Compos.* 36 (2013) 128–135. doi:10.1016/j.cemconcomp.2012.10.002.
- [18] M.A. Shirakawa, A.P. Werle, C.C. Gaylarde, K. Loh, V.M. John, Fungal and phototroph growth on fiber cement roofs and its influence on solar reflectance in a tropical climate, *Int. Biodeterior. Biodegradation.* 95 (2014) 1–6. doi:10.1016/j.ibiod.2013.12.003.
- [19] C. Ferrari, G. Santunione, A. Libbra, A. Muscio, E. Sgarbi, C. Siligardi, G.S. Barozzi, Review On The Influence Of Biological Deterioration On The Surface Properties Of Building Materials: Organisms, Materials, And Methods, *Int. J. Des. Nat. Ecodynamics.* 10 (2015) 21–39. doi:10.2495/DNE-V10-N1-21-39.
- [20] R. Paolini, M. Sleiman, M. Pedferri, M.V. Diamanti, TiO<sub>2</sub> alterations with natural aging: Unveiling the role of nitric acid on NIR reflectance, *Sol. Energy Mater. Sol. Cells.* 157 (2016) 791–797. doi:10.1016/j.solmat.2016.07.052.
- [21] P. Berdahl, H. Akbari, R. Levinson, W. a. Miller, Weathering of roofing materials – An overview, *Constr. Build. Mater.* 22 (2008) 423–433. doi:10.1016/j.conbuildmat.2006.10.015.
- [22] A.G. Mainini, T. Poli, R. Paolini, M. Zinzi, L. Vercesi, Transparent Multilayer ETFE Panels for Building Envelope: Thermal Transmittance Evaluation and Assessment of Optical and Solar Performance Decay due to Soiling, *Energy Procedia.* 48 (2014) 1302–1310. doi:10.1016/j.egypro.2014.02.147.
- [23] M.V. Diamanti, R. Paolini, M. Rossini, A.B. Aslan, M. Zinzi, T. Poli, M.P. Pedferri, Long term self-cleaning and photocatalytic performance of anatase added mortars exposed to the urban environment, *Constr. Build. Mater.* 96 (2015) 270–278. doi:10.1016/j.conbuildmat.2015.08.028.
- [24] M.V. Diamanti, B. Del Curto, M. Ormellese, M.P. Pedferri, Photocatalytic and self-cleaning activity of colored mortars containing TiO<sub>2</sub>, *Constr. Build. Mater.* 46 (2013) 167–174. doi:10.1016/j.conbuildmat.2013.04.038.
- [25] OMD, Osservatorio Meteorologico di Milano Duomo, (2016). <http://www.meteoduomo.it/> (accessed April 28, 2016).
- [26] R. Paolini, A. Zani, M. MeshkinKiya, V.L. Castaldo, A.L. Pisello, F. Antretter, T. Poli, F. Cotana, The hygrothermal performance of residential buildings at urban and rural sites: Sensible and latent energy loads and indoor environmental conditions, *Energy Build.* (2016). doi:10.1016/j.enbuild.2016.11.018.
- [27] ISO, ISO 9050 - Glass in building - Determination of light transmittance, solar direct transmittance, total solar energy transmittance, ultraviolet transmittance and related glazing factors, (2003).
- [28] ASTM, ASTM E 903-12. Standard Test Method for Solar Absorptance, Reflectance, and Transmittance of Materials Using Integrating Spheres, (2012). doi:10.1520/E0903-12.
- [29] A. Synnefa, A. Pantazaras, M. Santamouris, E.M.D. Bozonnet, M. Doya, M. Zinzi, A. Muscio, A. Libbra, C. Ferrari, V. Coccia, F. Rossi, D. Kolokotsa, Interlaboratory Comparison of Cool Roofing Material Measurement Methods, in: 34th AIVC Conf., Athens, Greece, 2013.
- [30] CEN, EN 15976. Flexible sheets for waterproofing. Determination of emissivity, (2011).
- [31] M. Rubin, J. Johnson, NFRC Interlaboratory Comparison on Optical Properties, Berkeley, CA, USA, 2007. <http://gaia.lbl.gov/btech/papers/501.pdf>.
- [32] ASTM, ASTM C1371-04a. Standard Test Method for Determination of Emittance of Materials Near Room Temperature Using Portable Emissometers, (2004).
- [33] F. Pini, C. Ferrari, A. Libbra, F. Leali, Robotic implementation of the slide method for measurement of the thermal emissivity of building elements, *Energy Build.* 114 (2016) 241–246. doi:10.1016/j.enbuild.2015.07.034.
- [34] R.W.G. Hunt, The Specification of Colour Appearance. I. Concepts and Terms, *Color Res. Appl.* 2 (1977) 55–68. doi:10.1002/col.5080020202.
- [35] ISO, ISO 11664. Colorimetry, (2007).
- [36] ASTM, ASTM C 1794 – 15. Standard Test Methods for Determination of the Water Absorption Coefficient by Partial Immersion, (2015). doi:10.1520/ C1794-15.
- [37] C. Feng, H. Janssen, Y. Feng, Q. Meng, Hygric properties of porous building materials: Analysis of measurement repeatability and reproducibility, *Build. Environ.* 85 (2015) 160–172. doi:10.1016/j.buildenv.2014.11.036.
- [38] C. Feng, H. Janssen, Hygric properties of porous building materials (II): Analysis of temperature

- influence, *Build. Environ.* 99 (2016) 107–118. doi:10.1016/j.buildenv.2016.01.016.
- [39] S. Roels, J. Carmeliet, H. Hens, O. Adan, H. Brocken, R. Cerny, Z. Pavlik, C. Hall, K. Kumaran, L. Pel, R. Plagge, Interlaboratory Comparison of Hygric Properties of Porous Building Materials, *J. Build. Phys.* 27 (2004) 307–325. doi:10.1177/1097196304042119.
- [40] R. Levinson, P. BERDAHL, A. Asefawberhe, H. AKBARI, Effects of soiling and cleaning on the reflectance and solar heat gain of a light-colored roofing membrane, *Atmos. Environ.* 39 (2005) 7807–7824. doi:10.1016/j.atmosenv.2005.08.037.
- [41] P. Caputo, G. Costa, S. Ferrari, A supporting method for defining energy strategies in the building sector at urban scale, *Energy Policy.* 55 (2013) 261–270. doi:10.1016/j.enpol.2012.12.006.
- [42] Governo Italiano, DM 26 giugno 2015. Applicazione delle metodologie di calcolo delle prestazioni energetiche e definizione delle prescrizioni e dei requisiti minimi degli edifici, *Gazzetta Ufficiale della Repubblica Italiana*, Roma, Italia, Italy, 2015.
- [43] MASEA Datenbank, (n.d.). <http://www.masea-ensan.de/> (accessed May 12, 2016).
- [44] ISO, ISO 9346. Hygrothermal performance of buildings and building materials - Physical quantities for mass transfer - Vocabulary, (2007).
- [45] UNI, UNI TS 11300-1. Energy Performance of Buildings—Part 1. Calculation of Energy Use for Space Heating and Cooling, (2014).
- [46] C. Dimitroulopoulou, Ventilation in European dwellings: A review, *Build. Environ.* 47 (2012) 109–125. doi:10.1016/j.buildenv.2011.07.016.
- [47] A. Holm, H.M. Kuenzel, K. Sedlbauer, The Hygrothermal Behaviour of Rooms : Combining Thermal Building Simulation and Hygrothermal Envelope Calculation, in: *Eighth Int. Build. Perform. Simul. Assoc. Conf.*, Eindhoven, Netherlands, 2003: pp. 499–506. [http://www.ibpsa.org/%5Cproceedings%5CBS2003%5CBS03\\_0499\\_506.pdf](http://www.ibpsa.org/%5Cproceedings%5CBS2003%5CBS03_0499_506.pdf).
- [48] F. Antretter, F. Sauer, T. Schöpfer, A. Holm, Validation of a hygrothermal whole building simulation software, in: *12th Conf. Int. Build. Perform. Simul. Assoc.*, Sydney, Australia, 2011: pp. 1694–1701. [http://www.ibpsa.org/proceedings/bs2011/p\\_1554.pdf](http://www.ibpsa.org/proceedings/bs2011/p_1554.pdf).
- [49] H.M. Künel, A. Holm, D. Zirkelbach, A.N. Karagiozis, Simulation of indoor temperature and humidity conditions including hygrothermal interactions with the building envelope, *Sol. Energy.* 78 (2005) 554–561. doi:10.1016/j.solener.2004.03.002.
- [50] D. Allinson, M. Hall, Hygrothermal analysis of a stabilised rammed earth test building in the UK, *Energy Build.* 42 (2010) 845–852. doi:10.1016/j.enbuild.2009.12.005.
- [51] F. Antretter, C. Mitterer, S.M. Young, Use of moisture-buffering tiles for indoor climate stability under different climatic requirements, *HVAC R Res.* 18 (2012) 275–282. doi:10.1080/10789669.2012.645399.
- [52] B. Daniotti, R. Paolini, F.R. Cecconi, *Durability of Building Materials and Components*, Springer Berlin Heidelberg, Berlin, Heidelberg, 2013. doi:10.1007/978-3-642-37475-3.
- [53] B. Amaro, D. Saraiva, J. de Brito, I. Flores-Colen, Inspection and diagnosis system of ETICS on walls, *Constr. Build. Mater.* 47 (2013) 1257–1267. doi:10.1016/j.conbuildmat.2013.06.024.
- [54] B. Daniotti, F.R. Cecconi, R. Paolini, G. Cocchetti, R. Galliano, A. Cornaggia, Multi-Physics Modelling for Durability Evaluation of ETICS, in: M. Quattrone, V.M. John (Eds.), *XIII Int. Conf. Durab. Build. Mater. Components*, São Paulo, Brazil, 2014: pp. 514–521.
- [55] EAE (European Association for External Thermal Insulation Systems), European guideline for the application of ETICS, (2011). <http://www.ea-etics.eu/content/pictures/home/ETICS.pdf>.
- [56] R.G. Kuehni, R.T. Marcus, An Experiment in Visual Scaling of Small Color Differences, *Color Res. Appl.* 4 (1979) 83–91. doi:10.1111/j.1520-6378.1979.tb00094.x.
- [57] R.R. Seghi, E.R. Hewlett, J. Kim, Visual and Instrumental Colorimetric Assessments of Small Color Differences on Translucent Dental Porcelain, *J. Dent. Res.* 68 (1989) 1760–1764. doi:10.1177/00220345890680120801.
- [58] R.D. Douglas, T.J. Steinhauer, A.G. Wee, Intraoral determination of the tolerance of dentists for perceptibility and acceptability of shade mismatch, *J. Prosthet. Dent.* 97 (2007) 200–208. doi:10.1016/j.prosdent.2007.02.012.
- [59] R.M. Espinosa-Marzal, G.W. Scherer, Impact of in-pore salt crystallization on transport properties, *Environ. Earth Sci.* 69 (2013) 2657–2669. doi:10.1007/s12665-012-2087-z.
- [60] W.P.. Dias, Reduction of concrete sorptivity with age through carbonation, *Cem. Concr. Res.* 30 (2000) 1255–1261. doi:10.1016/S0008-8846(00)00311-2.
- [61] R. Levinson, H. Akbari, Effects of composition and exposure on the solar reflectance of portland cement concrete, *Cem. Concr. Res.* 32 (2002) 1679–1698. doi:10.1016/S0008-8846(02)00835-9.
- [62] A.L. Pisello, R. Paolini, M.V. Diamanti, E. Fortunati, V.L. Castaldo, L. Torre, Nanotech-Based Cool Materials for Building Energy Efficiency, in: *Nano Biotech Based Mater. Energy Build. Effic.*, Springer

- International Publishing, Cham, 2016: pp. 245–278. doi:10.1007/978-3-319-27505-5\_9.
- [63] A.M. Baldrige, S.J. Hook, C.I. Grove, G. Rivera, The ASTER spectral library version 2.0, *Remote Sens. Environ.* 113 (2009) 711–715. doi:10.1016/j.rse.2008.11.007.
- [64] S. Kotthaus, T.E.L. Smith, M.J. Wooster, C.S.B. Grimmond, Derivation of an urban materials spectral library through emittance and reflectance spectroscopy, *ISPRS J. Photogramm. Remote Sens.* 94 (2014) 194–212. doi:10.1016/j.isprsjprs.2014.05.005.
- [65] P. Berdahl, H. Akbari, L.S. Rose, Aging of reflective roofs: soot deposition., *Appl. Opt.* 41 (2002) 2355–60. <http://www.ncbi.nlm.nih.gov/pubmed/12003230>.
- [66] T.C. Bond, D.G. Streets, K.F. Yarber, S.M. Nelson, J. Woo, Z. Klimont, A technology-based global inventory of black and organic carbon emissions from combustion, *J. Geophys. Res.* 109 (2004) D14203. doi:10.1029/2003JD003697.
- [67] N. Aste, R.S. Adhikari, J. Compostella, C. Del Pero, Energy and environmental impact of domestic heating in Italy: Evaluation of national NO<sub>x</sub> emissions, *Energy Policy.* 53 (2013) 353–360. doi:10.1016/j.enpol.2012.10.064.
- [68] T. Novakov, S. Menon, T.W. Kirchstetter, D. Koch, J.E. Hansen, Aerosol organic carbon to black carbon ratios: Analysis of published data and implications for climate forcing, *J. Geophys. Res.* 110 (2005) D21205. doi:10.1029/2005JD005977.
- [69] L. Ferrero, M. Castelli, B.S. Ferrini, M. Moscatelli, M.G. Perrone, G. Sangiorgi, L. D’Angelo, G. Rovelli, B. Moroni, F. Scardazza, G. Močnik, E. Bolzacchini, M. Petitta, D. Cappelletti, Impact of black carbon aerosol over Italian basin valleys: high-resolution measurements along vertical profiles, radiative forcing and heating rate, *Atmos. Chem. Phys.* 14 (2014) 9641–9664. doi:10.5194/acp-14-9641-2014.
- [70] ARPA Lombardia, Air quality data of ARPA Lombardia, Agenzia Regionale per la Protezione Ambientale della Lombardia (Environmental Protection Agency of Lombardia region, Italy), (2015). <http://www2.arpalombardia.it/>.
- [71] S. Kaur, M.J. Nieuwenhuijsen, R.N. Colvile, Fine particulate matter and carbon monoxide exposure concentrations in urban street transport microenvironments, *Atmos. Environ.* 41 (2007) 4781–4810. doi:10.1016/j.atmosenv.2007.02.002.
- [72] S. Di Sabatino, R. Buccolieri, B. Pulvirenti, R.E. Britter, Flow and Pollutant Dispersion in Street Canyons using FLUENT and ADMS-Urban, *Environ. Model. Assess.* 13 (2008) 369–381. doi:10.1007/s10666-007-9106-6.
- [73] C.J. Hopfe, J.L.M. Hensen, Uncertainty analysis in building performance simulation for design support, *Energy Build.* 43 (2011) 2798–2805. doi:10.1016/j.enbuild.2011.06.034.
- [74] M. Manfren, N. Aste, R. Moshksar, Calibration and uncertainty analysis for computer models – A meta-model based approach for integrated building energy simulation, *Appl. Energy.* 103 (2013) 627–641. doi:10.1016/j.apenergy.2012.10.031.